**Earth Sciences**
2021; 10(6): 325-331
http://www.sciencepublishinggroup.com/j/earth
doi: 10.11648/j.earth.20211006.18
ISSN: 2328-5974 (Print); ISSN: 2328-5982 (Online)

# Geochemical Characteristics and Genesis of Biotite Monzogranite in Southeastern Guangxi Province, South China

**Tian Mengyu[1], Di Yongjun[1, *], Li Shusheng[2, *], Zhang Sheng[3]**

[1]School of Earth Science and Mineral Resources, China University of Geosciences, Beijing, China

[2]Geology Team No. 4 of Guangxi Zhuang Autonomic Region, Nanning, China

[3]Remote Sensing Center of Guangxi, Nanning, China

## Email address:

diyongjun@cugb.edu.cn (Di Yongjun), 827661228@qq.com (Li Shusheng)

[*]Corresponding author

## To cite this article:

Tian Mengyu, Di Yongjun, Li Shusheng, Zhang Sheng. Geochemical Characteristics and Genesis of Biotite Monzogranite in Southeastern Guangxi Province, South China. *Earth Sciences*. Vol. 10, No. 6, 2021, pp. 325-331. doi: 10.11648/j.earth.20211006.18

**Received**: November 19, 2021; **Accepted**: December 7, 2021; **Published**: December 24, 2021

**Abstract:** The South China Block experienced intense tectonic–magmatic evolution during the Indosinian period, which was recorded by Indosinian granite and has attracted numerous researchers. This paper presents data on the geochronology and geochemistry of Darongshan biotite monzogranite. LA–ICP–MS U–Pb zircon analyses yielded a weighted average age of 250.1±1.6 Ma, which represents the magma crystallization age of the Early Triassic. According to petrographic observation, the main diagenetic minerals of Darongshan biotite monzogranite are quartz, K-feldspar, plagioclase, biotite, and small amounts of cordierite, tourmaline, and garnet. Darongshan biotite monzogranite is aluminum-rich and high in silica. It shows weak negative Eu anomalies (δEu=0.13–0.57) and depleted HREEs. Darongshan biotite monzogranite exhibits significant negative anomalies of high field strength elements (HFSE, e.g., Nb, Ta, Ti, and P) and positive anomalies of large-ion lithophile elements (LILE, e.g., Rb, Th, U, and Pb). Geochemical analyses suggested that Darongshan biotite monzogranite has undergone highly differentiated evolution. According to this study, Darongshan biotite monzogranite is an S-type granite, and its source material developed from the remelting of ancient crustal material. The Darongshan biotite monzogranite granite formed in the island arc environment of oceanic subduction and orogenic stage, further confirming the geological records of the remaining oceanic basin in Qinfang.

**Keywords:** Zircon U-Pb, Geochemistry, Biotite Monzogranite, South China

## 1. Introduction

The Caledonian orogenic event resulted in the collision of the Yangtze and Cathaysia plates to form the unified South China Block [22]. Subsequently, the South China Block experienced three main tectonic–magmatic stages: the Caledonian (490–390 Ma), Indosinian (257–200 Ma), and Yanshanian (200–65 Ma) [6, 16, 20]. Over the past 20 years, the tectonic history of the Indosinian stage in South China has become a hot research topic. The multi-stage orogenic movement from the Neoproterozoic to Mesozoic in southeastern Guangxi was accompanied by strong intracontinental compression and the development of a large number of granite formations [2]. However, there is still a controversy about the evolutionary history of the Darongshan granitic pluton in southeastern Guangxi Province. Some researchers believe that the granitic pluton is a typical granite formed by deep emplacement that occurred in the middle–late Triassic [12], while others believe it was formed as the result of a collision between the Hercynian and Indosinian Plates [5]. Given these differing explanations, it is necessary to investigate the formation age, petrogenesis, and tectonic environment of Darongshan granitic pluton to better understand the tectonic–magmatic evolutionary history of South China.

In this paper, we present the crystallization age and geochemical characteristics of the Darongshan biotite monzogranite and further discuss its evolutionary history. These new data are important for understanding the tectonic–magmatic evolutionary history of the Indosinian stage in South China.

## 2. Geological Setting and Samples

The study area is located at the southwest end of the famous Qinhang tectonic fault zone in China, southeast of the Guangxi Zhuang Autonomous Region, and belongs to the Darongshan-Shiwandashan granite belt region. It is an important component of Hercynian-Indosinian granite in eastern Guangxi as well as an important part of the orogenic process of the Yangtze and Cathaysia plate collision [22]. The Darongshan-Shiwandashan granite belt in southeastern Guangxi runs from northeast to southwest and is approximately 400 km long and 20–80 km wide, with a total exposed area exceeding 10,000 km$^2$. It extends from the vicinity of Wuzhou in the north to the southwest of the Beibu Gulf and may extend further into Vietnam. The Darongshan-Shiwandashan granite belt is primarily composed of the Darongshan, Pubei, Taima, and Jiuzhou rock masses, which contain granitoid rocks with varying occurrences and structures. Because of common source material and shared evolutionary history, this area is collectively known as the "Darongshan granite suite" (Figure 1).

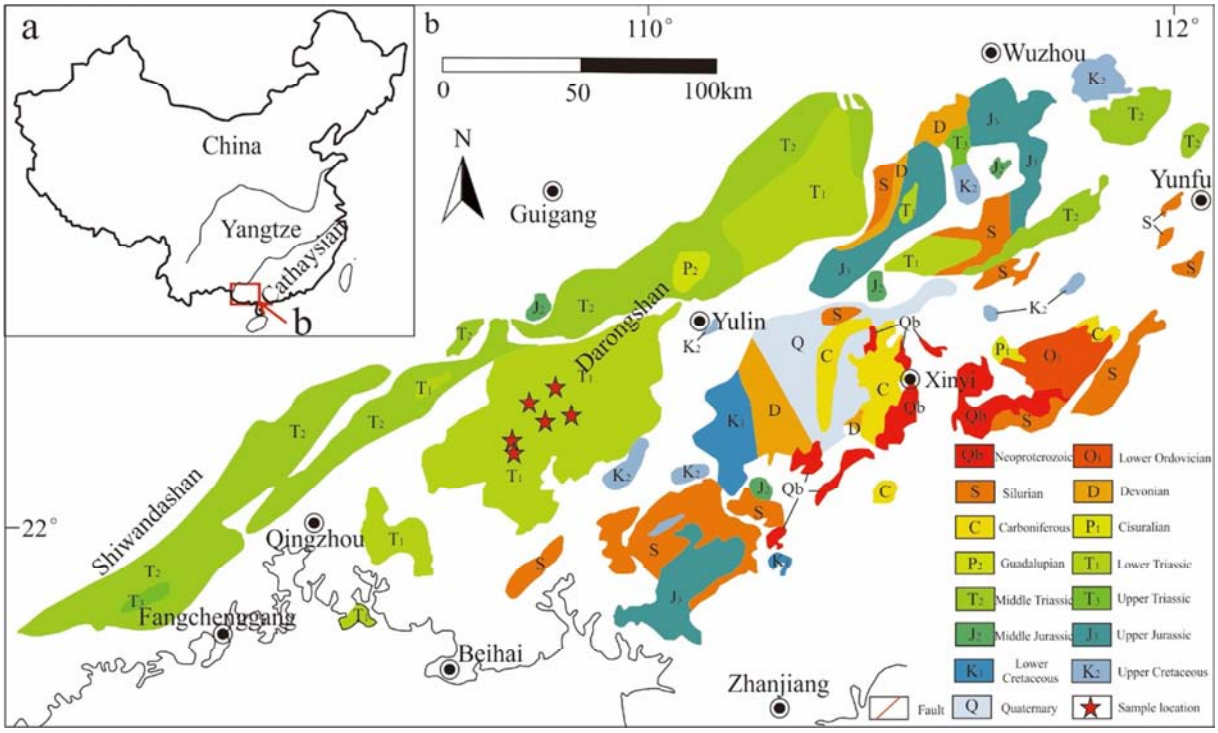


***Figure 1.*** *Geological sketch map of the Darongshan granite mass in southeastern Guangxi.*

The Darongshan biotite monzogranite is gray with gradational contacts between phases. The outer phase is medium- to fine-grained, with a granophyric texture and massive structure. The major rock-forming minerals are quartz (20–25%), K-feldspar (15–20%), plagioclase (20–25%), and biotite (10–15%) with minor amounts of cordierite. Anhedral quartz ranges in size from 1 to 3.5 mm, and quartz infuses feldspar grains (Figures 2a–d). Subhedral K-feldspar phenocrysts range in size from 1.5 to 5.5 mm; their surfaces appear dirty and are probably kaolinized (Figures 2c–d). Plagioclase is white with a broad plate shape that exhibits albite twinning. Subhedral plagioclases range in size from 2 to 6 mm, and secondary alteration is mainly due to kaolinization (Figures 2a, b, e, f). Biotite is dark brown with a flakey structure and ranges in size from 1.5 mm to 4.5 mm. It is mainly distributed between feldspar and quartz particles and tends to agglomerate. (Figures 2a, b, e, f). Cordierite appears irregularly granular, and serpentinization is its main alteration type. Additionally, Darongshan biotite monzogranite contains very small amounts of tourmaline and other minerals.

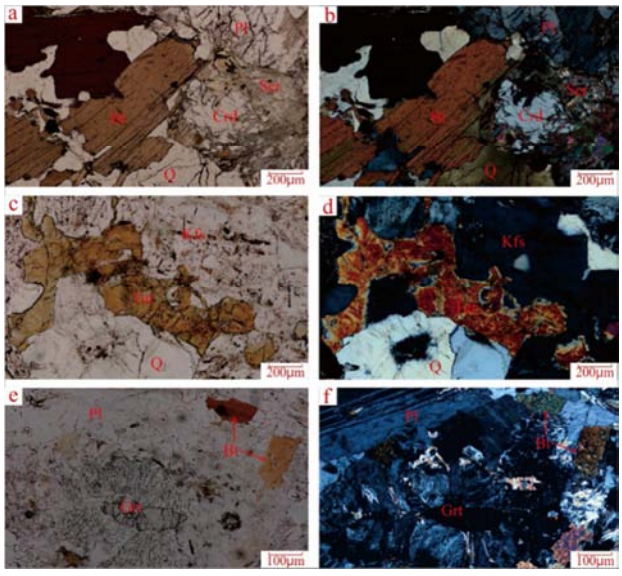


***Figure 2.*** *Micrographs of biotite monzogranite samples of Darongshan granite.*

# 3. Analytical Methods

A fresh sample of Darongshan biotite monzogranite (YK037) was selected for zircon dating. Zircon sorting was performed by Langfang Geoscience Exploration Technology Service Co., Ltd. Zircon target preparation, cathodoluminescence micrography (CL), and LA-ICP-MS zircon U-Pb dating were completed by Beijing Zircon Linghang Technology Co., Ltd. The zircon was photographed using a JSM6510 (JEOL Corporation, Japan) scanning electron microscope. Zircon dating analysis was performed using a Finnigan Neptune LA-ICP-MS and the accompanying New Wave UP213 laser ablation system.

The analysis of major, trace, and rare earth elements of Darongshan biotite monzogranite was completed at Peking University's Key Laboratory of Orogenic Belts and Crustal Evolution. The main elements were measured using the Flax method and analyzed using a scanning wavelength dispersive X-ray fluorescence spectrometer (ARLADVANTXP+) with an error of less than 5%. Trace elements and rare earth elements were analyzed by ICP-MS, and samples were dissolved in high-pressure tanks (instrument model Finnigan MAT Element2) before testing, with an error of less than 10%.

# 4. Results

### *4.1. Zircon U–Pb Ages*

Zircon from Darongshan biotite monzogranite (YK037) was analyzed at twenty-five points (Table 1). As Table 1 shows, the samples ranged widely in age (1364-206 Ma), indicating that some zircons may have originated from Caledonian or older magmatic zircons, while the others may have undergone different degrees of metamorphism. However, the dating results showed that zircons that originated between 256 and 247 Ma had good crystal shapes and clear growth bands with typical magmatic characteristics. The $^{206}Pb/^{238}U$ age of the ten spot analyses ranged from 256 ± 3 to 247 ± 3 Ma (Table 1); these are plotted within a small field along the Concordia line (Figure 3). Ten spots yielded a $^{206}Pb/^{238}U$ age of 250.1±1.6Ma (MSWD=1.8). It can be explained that the crystallization age of the Darongshan biotite monzogranite. This is similar to the results reported by Jiao et al. (SIMS zircon U-Pb ages of 248.5 ± 1.7 and 250.2 ± 1.8 Ma) [4].

***Table 1.*** *Zircon LA-ICP-MS U-Pb analytical results.*

| Spot | $w_B/10^{-6}$ | | | Isotope ratio | | | | | | Age/Ma | | | | | |
|---|---|---|---|---|---|---|---|---|---|---|---|---|---|---|---|
| | Pb | Th | U | $^{207}Pb/^{206}Pb$ | 1σ | $^{207}Pb/^{235}U$ | 1σ | $^{206}Pb/^{238}U$ | 1σ | $^{207}Pb/^{206}Pb$ | 1σ | $^{207}Pb/^{235}U$ | 1σ | $^{206}Pb/^{238}U$ | 1σ |
| 1 | 69 | 81 | 269 | 0.1814 | 0.0032 | 5.7783 | 0.4866 | 0.2226 | 0.0159 | 2666 | 29 | 1943 | 73 | 1296 | 84 |
| 2 | 117 | 365 | 343 | 0.0992 | 0.0014 | 3.2216 | 0.0521 | 0.2356 | 0.0021 | 1609 | 26 | 1462 | 13 | 1364 | 11 |
| 3 | 12 | 89 | 270 | 0.0554 | 0.0017 | 0.2978 | 0.0098 | 0.0390 | 0.0004 | 428 | 64 | 265 | 8 | 247 | 3 |
| 4 | 15 | 107 | 320 | 0.0561 | 0.0017 | 0.3052 | 0.0100 | 0.0394 | 0.0005 | 457 | 67 | 270 | 8 | 249 | 3 |
| 5 | 17 | 51 | 380 | 0.0514 | 0.0019 | 0.2857 | 0.0094 | 0.0405 | 0.0004 | 257 | 83 | 255 | 7 | 256 | 2 |
| 6 | 28 | 106 | 194 | 0.0744 | 0.0021 | 1.1557 | 0.0387 | 0.1124 | 0.0017 | 1054 | 56 | 780 | 18 | 687 | 10 |
| 7 | 53 | 79 | 324 | 0.1508 | 0.0027 | 2.5076 | 0.0644 | 0.1206 | 0.0020 | 2355 | 30 | 1274 | 19 | 734 | 11 |
| 8 | 20 | 130 | 446 | 0.0565 | 0.0016 | 0.3058 | 0.0082 | 0.0394 | 0.0004 | 472 | 61 | 271 | 6 | 249 | 2 |
| 9 | 16 | 90 | 286 | 0.0570 | 0.0015 | 0.3688 | 0.0109 | 0.0469 | 0.0007 | 494 | 57 | 319 | 8 | 295 | 4 |
| 10 | 15 | 79 | 356 | 0.0567 | 0.0016 | 0.2958 | 0.0096 | 0.0378 | 0.0005 | 480 | 63 | 263 | 7 | 239 | 3 |
| 11 | 18 | 56 | 376 | 0.0531 | 0.0016 | 0.3039 | 0.0087 | 0.0417 | 0.0004 | 332 | 69 | 269 | 7 | 263 | 2 |
| 12 | 70 | 55 | 821 | 0.0671 | 0.0014 | 0.7156 | 0.0164 | 0.0774 | 0.0008 | 839 | 42 | 548 | 10 | 481 | 5 |
| 13 | 23 | 47 | 95 | 0.0836 | 0.0020 | 2.2387 | 0.0532 | 0.1947 | 0.0020 | 1283 | 46 | 1193 | 17 | 1147 | 11 |
| 14 | 19 | 105 | 414 | 0.0573 | 0.0018 | 0.3199 | 0.0107 | 0.0405 | 0.0005 | 502 | 69 | 282 | 8 | 256 | 3 |
| 15 | 24 | 99 | 542 | 0.0985 | 0.0023 | 0.4683 | 0.0111 | 0.0345 | 0.0003 | 1598 | 43 | 390 | 8 | 219 | 2 |
| 16 | 29 | 272 | 667 | 0.0620 | 0.0013 | 0.3131 | 0.0075 | 0.0366 | 0.0004 | 676 | 43 | 277 | 6 | 232 | 2 |
| 17 | 14 | 96 | 311 | 0.0562 | 0.0017 | 0.3033 | 0.0096 | 0.0392 | 0.0004 | 457 | 67 | 269 | 7 | 248 | 3 |
| 18 | 27 | 79 | 451 | 0.0632 | 0.0014 | 0.4891 | 0.0206 | 0.0557 | 0.0017 | 722 | 48 | 404 | 14 | 349 | 10 |
| 19 | 12 | 60 | 280 | 0.0543 | 0.0019 | 0.2927 | 0.0105 | 0.0392 | 0.0005 | 383 | 78 | 261 | 8 | 248 | 3 |
| 20 | 16 | 38 | 369 | 0.0523 | 0.0016 | 0.2839 | 0.0095 | 0.0393 | 0.0005 | 302 | 70 | 254 | 8 | 249 | 3 |
| 21 | 32 | 92 | 898 | 0.0552 | 0.0013 | 0.2470 | 0.0058 | 0.0325 | 0.0003 | 417 | 56 | 224 | 5 | 206 | 2 |
| 22 | 20 | 46 | 482 | 0.0539 | 0.0018 | 0.2897 | 0.0100 | 0.0390 | 0.0005 | 365 | 69 | 258 | 8 | 247 | 3 |
| 23 | 142 | 408 | 861 | 0.0767 | 0.0011 | 1.4197 | 0.0363 | 0.1345 | 0.0032 | 1122 | 26 | 897 | 15 | 813 | 18 |
| 24 | 46 | 92 | 1054 | 0.0544 | 0.0012 | 0.3081 | 0.0086 | 0.0411 | 0.0007 | 387 | 48 | 273 | 7 | 259 | 4 |
| 25 | 14 | 97 | 309 | 0.0552 | 0.0016 | 0.3012 | 0.0088 | 0.0397 | 0.0005 | 420 | 67 | 267 | 7 | 251 | 3 |

### *4.2. Geochemical Characteristics*

The abundances of major and trace elements in the Darongshan biotite monzogranite are shown in Table 2. The rocks contained a range of $SiO_2$, from 66.90 to 72.98 wt.%, and were classified as granite (Figure 4a). They exhibited high concentrations of $Al_2O_3$ (13.74–16.44 wt.%), CaO (0.11–1.41 wt.%), MgO (0.07–2.13 wt.%), $TiO_2$ (0.03–0.47 wt.%), MnO (0.01–0.03 wt.%) and $P_2O_5$ (0.01–0.27 wt.%), as well as $K_2O+Na_2O$ (5.79–12.65 wt.%) and $K_2O/Na_2O$ ratios (0.21–0.78). These samples were strongly peraluminous with A/CNK (molar $Al_2O_3/CaO+Na_2O+K_2O$) ranging from 1.10 to 1.83 and A/NK (molar $Al_2O_3/Na_2O+K_2O$) from 1.14 to 2.37 (Figure 4b).

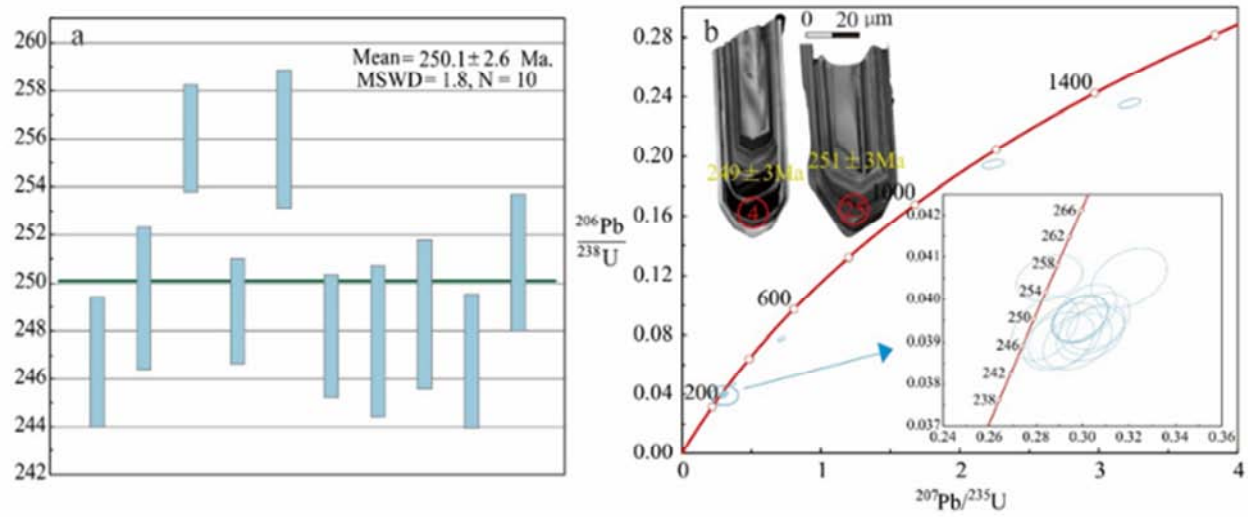


***Figure 3.*** *Zircon site map and U-Pb age harmonic map of Darongshan biotite monzogranite.*

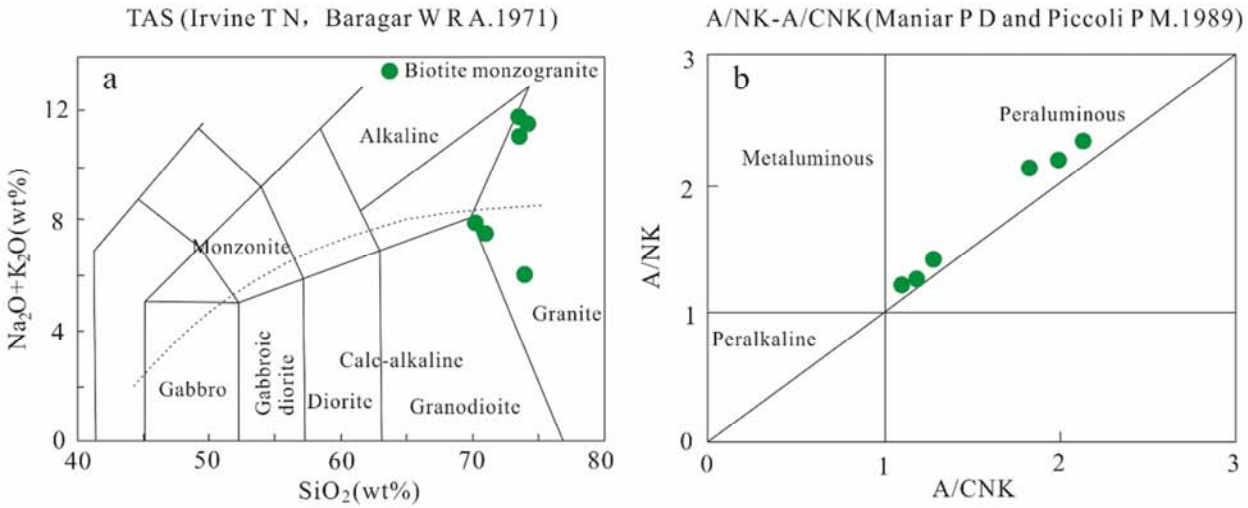


***Figure 4.*** *$SiO_2$-$K_2O$ and A/NK-A/CNK diagrams for Darongshan biotite monzogranite. A = $Al_2O_3$, N=$Na_2O$, K = $K_2O$, C = CaO (all in molar proportions) [3, 9].*

The total rare earth element (REE) contents of the outer and inner phase samples ranged from 118.65 to 243.94 ppm, with LREE/HREE ratio range of 3.48–16.20 (Table 2). Our samples showed high similarity of chondrite normalized REE patterns, which showed a right-leaning HREE pattern and weak negative Eu anomalies (δEu = 0.13–0.57). Normalized to a primitive mantle, all samples for the Darongshan biotite monzogranite exhibited similar trace element patterns, with substantial negative anomalies for HFSE (Nb, Ta, Ti, and P) and positive anomalies of LILE (Rb, Th, U, and Pb) (Figure 5).

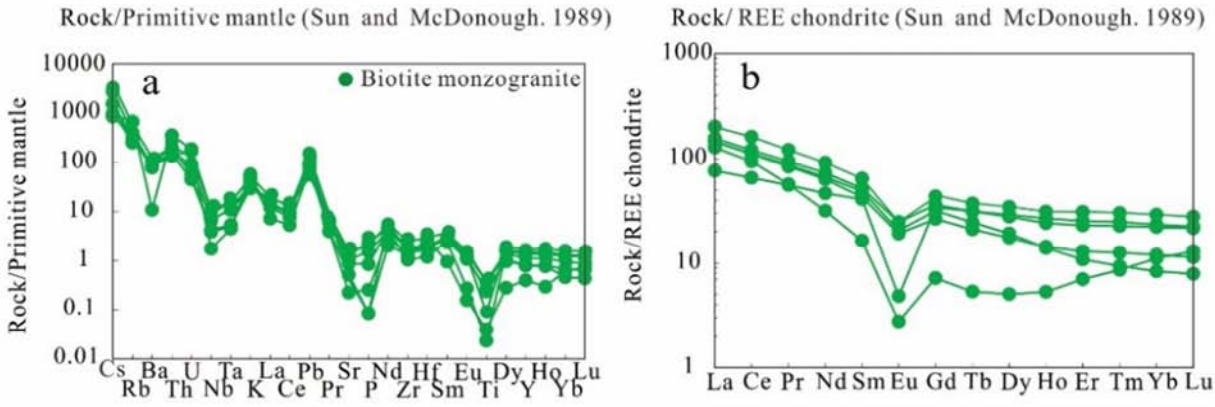


***Figure 5.*** *Rock/Primitive mantle diagrams and Rock/REE chondrite diagrams for Darongshan biotite monzogranite [13].*

***Table 2.*** *Major, trace and rare earth elements analytical results.*

| Major and trace oxides in % | YK027 | YK028 | YK030 | YK031 | YK033 | YK034 |
|---|---|---|---|---|---|---|
| $SiO_2$ | 66.9 | 72.98 | 67.8 | 71.12 | 70.8 | 69.93 |
| $TiO_2$ | 0.47 | 0.3 | 0.33 | 0.05 | 0.03 | 0.11 |
| $Al_2O_3$ | 16.44 | 13.74 | 16.47 | 14.56 | 15.49 | 14.4 |
| $Fe_2O_3$ | 1.13 | 0.88 | 1.1 | 0.12 | 0.09 | 0.36 |
| FeO | 1.66 | 1.23 | 1.62 | 0.23 | 0.17 | 0.66 |
| MnO | 0.02 | 0.02 | 0.03 | 0.02 | 0.01 | 0.01 |
| MgO | 2.13 | 1.76 | 2.2 | 0.07 | 0.27 | 0.24 |
| CaO | 1.41 | 0.7 | 0.61 | 0.11 | 0.26 | 0.53 |
| $Na_2O$ | 5.32 | 3.24 | 4.92 | 9.39 | 7.8 | 10.45 |
| $K_2O$ | 2.25 | 2.54 | 2.64 | 3.27 | 3.91 | 2.16 |
| $P_2O_5$ | 0.27 | 0.1 | 0.18 | 0.01 | 0.03 | 0.01 |
| LOI | 1.38 | 1.97 | 1.4 | 0.6 | 0.64 | 0.6 |
| Sum | 99.38 | 99.46 | 99.3 | 99.55 | 99.5 | 99.46 |
| A/CNK | 1.83 | 2.12 | 2.01 | 1.14 | 1.29 | 1.1 |
| Cs | 10.88 | 6.82 | 19.02 | 6.4 | 5.96 | 10.88 |
| Rb | 177.78 | 153.42 | 218.24 | 376 | 226.08 | 143.65 |
| Ba | 504.71 | 649.76 | 535.28 | 68.85 | 542.98 | 641.62 |
| Th | 19.62 | 23.94 | 18.24 | 42.67 | 16.54 | 18.2 |
| U | 4.25 | 2.7 | 4.41 | 8.93 | 8.02 | 2.14 |
| Nb | 16.83 | 9.11 | 15.23 | 24.71 | 4.14 | 9.95 |
| Ta | 1.42 | 0.66 | 1.57 | 2.18 | 0.6 | 0.72 |
| Pb | 27.66 | 29.66 | 27.87 | 46.49 | 22.49 | 15.51 |
| Sr | 118.6 | 78.92 | 94.8 | 46.79 | 20.09 | 37.03 |
| Zr | 138.35 | 124.53 | 78.5 | 99.01 | 99.09 | 180.85 |
| Hf | 4.1 | 3.69 | 2.47 | 5.5 | 4.76 | 6.06 |
| Y | 38.1 | 22.24 | 22.51 | 11.21 | 41.5 | 46.93 |
| La | 36.96 | 34.58 | 34.37 | 30.41 | 18.24 | 47.88 |
| Ce | 74.22 | 68.76 | 68 | 57.77 | 40.18 | 98.3 |
| Pr | 8.97 | 8.33 | 8.02 | 5.42 | 5.33 | 11.52 |
| Nd | 34.12 | 31.15 | 29.73 | 14.87 | 21.87 | 42.61 |
| Sm | 8.01 | 7.49 | 6.6 | 2.52 | 6.26 | 9.86 |
| Eu | 1.44 | 1.19 | 1.11 | 0.16 | 0.28 | 1.3 |
| Gd | 7.45 | 6.51 | 5.44 | 1.48 | 7.02 | 8.97 |
| Tb | 1.17 | 0.92 | 0.79 | 0.2 | 1.17 | 1.4 |
| Dy | 7.09 | 4.87 | 4.45 | 1.28 | 7.41 | 8.79 |
| Ho | 1.37 | 0.79 | 0.81 | 0.3 | 1.52 | 1.77 |
| Er | 3.8 | 1.79 | 2.15 | 1.16 | 4.2 | 5.13 |
| Tm | 0.58 | 0.24 | 0.32 | 0.22 | 0.63 | 0.77 |
| Yb | 3.76 | 1.42 | 2.05 | 1.89 | 3.99 | 4.94 |
| Lu | 0.55 | 0.2 | 0.29 | 0.33 | 0.57 | 0.71 |
| ∑REE | 189.49 | 168.25 | 164.14 | 118 | 118.65 | 243.94 |
| LREE | 163.73 | 151.51 | 147.84 | 111.14 | 92.15 | 211.46 |
| HREE | 25.76 | 16.74 | 16.3 | 6.86 | 26.5 | 32.48 |
| LREE/HREE | 6.36 | 9.05 | 9.07 | 16.20 | 3.48 | 6.51 |
| δEu | 0.57 | 0.52 | 0.57 | 0.26 | 0.13 | 0.42 |
| $(T_{Zr})$°C | 689 | 796 | 744 | 703 | 722 | 735 |

# 5. Discussion

## *5.1. Petrogenesis*

### *5.1.1. Genetic Type*

Granites were mainly formed in the extensional environments of subduction, collision, and post-collision orogenic stages. Genetic types of granites can be divided into A, M, I, and S types [10] based on their sources and natures. Tourmaline, garnet, and cordierite were observed in thin sections in both the outer and inner phase samples of the Darongshan biotite monzogranite. The A/CNK values were all higher than 1.1 (from 1.10 to 2.12), resembling those of typical S-type granites [1]. The $(Al_2O_3–(K_2O+Na_2O))–CaO–(Fe_2O_3+MgO)$ discrimination diagram further indicates that Darongshan biotite monzogranite is an S-type granite and is consistent with Nali granodiorite from the southeast Guangxi region (Figure 6a) [7]. In the Rb/Sr-Rb/Ba diagram, all samples belonged to the clay-rich crustal sources (Figure 6b), indicating that the source material of Darongshan granite was derived from the remelting of ancient crust-derived materials.

### *5.1.2. Origin*

Previous experimental studies have shown that zircon exists widely in granitic rocks; zircon saturation thermometers are important for identifying crustal melt granites [14]. Zircon is a secondary mineral that crystallizes earlier in granitic magmatic systems. Therefore, the saturation temperature of zircon can be used to approximate the liquidus temperature of granitic rocks. Our samples produced zircon saturation temperatures ($T_{Zr}$) ranging from 689–796°C (Table 2), based on the Harrison and Watson (1983) method. These observations provide evidence that Darongshan biotite monzogranite may have been formed by the reaction of deep magma with clay-rich rocks in the crust during the rising process.

Chemical analyses showed that the Late Permian granitoids are classified as alkali-calcic rocks and are characterized by enrichment in light rare earth elements (LREEs), large ion lithophile elements (LILEs), and depletion of heavy rare earth elements (HREEs), high field strength elements (HFSEs), Ba, and Sr, which is typical of low Ba-Sr crust-derived granites. The original Nb/Ta value of the mantle is generally between 15.50 and 19.50 [8], while the average value of the continental crust is approximately 11. The Nb/Ta value range of the Darongshan biotite monzogranite is between 6.9 and 13.82 (average 11.24). These values are within the range of the continental crust; the average value is even closer to that of the continental crust, which demonstrates that granite and continental crust have similar magmatic origins. Taylor believed higher Rb/Sr ratio values in granite indicated source rock primarily originating from the upper crust [15]. The Rb/Sr values of the samples in this study ranged from 1.50 to 11.25 (average 4.82), which are much higher than both the upper crust value in China (0.31) and the global upper crust average (0.32). These results, therefore, indicate that the source rock of Darongshan biotite monzogranite may have originated from the upper continental crust.

## *5.2. Tectonic Setting*

Our study showed that the U-Pb age of Darongshan biotite monzogranite was 250.1±1.6Ma, indicating that it was formed in the Early Triassic. The dynamic geotectonic history of this period has been a controversial topic in geology. For example, the Indosinian granites in South China may be the products of the northward subduction of the Paleo-Pacific Plate [6]. Granite formation may have been the result of the Emeishan mantle plume and the Indosinian tectono-magmatism in southeast Guangxi [4]. Yet another explanation is that the formation of Indosinian granites in

Guangxi may be related to the closure of the Paleotethys Ocean Basin [17]. All of our samples were within the range of volcanic arc granites (VAG) and syn-collision granites (Syn-COLG) (Figures 6c, d). These findings were combined with regional geological characteristics and evidence of arc-related volcanogenic sediments that were found in Youjiang Basin during 261-247 Ma [19]. Also, arc granites and volcanic rocks were found in southeast Guangxi during 250–246 Ma [18]. Therefore, we concluded that the Darongshan biotite monzogranite was formed in an island arc environment under oceanic subduction in the early Indosinian, which further confirms the geological records of the remaining oceanic basin in Qinfang. However, further study of isotope geochemistry, sedimentology, and mineralogy is still needed to understand the Indosinian tectonic setting in southeastern Guangxi and the exact time of the Qinfang residual ocean basin closure.

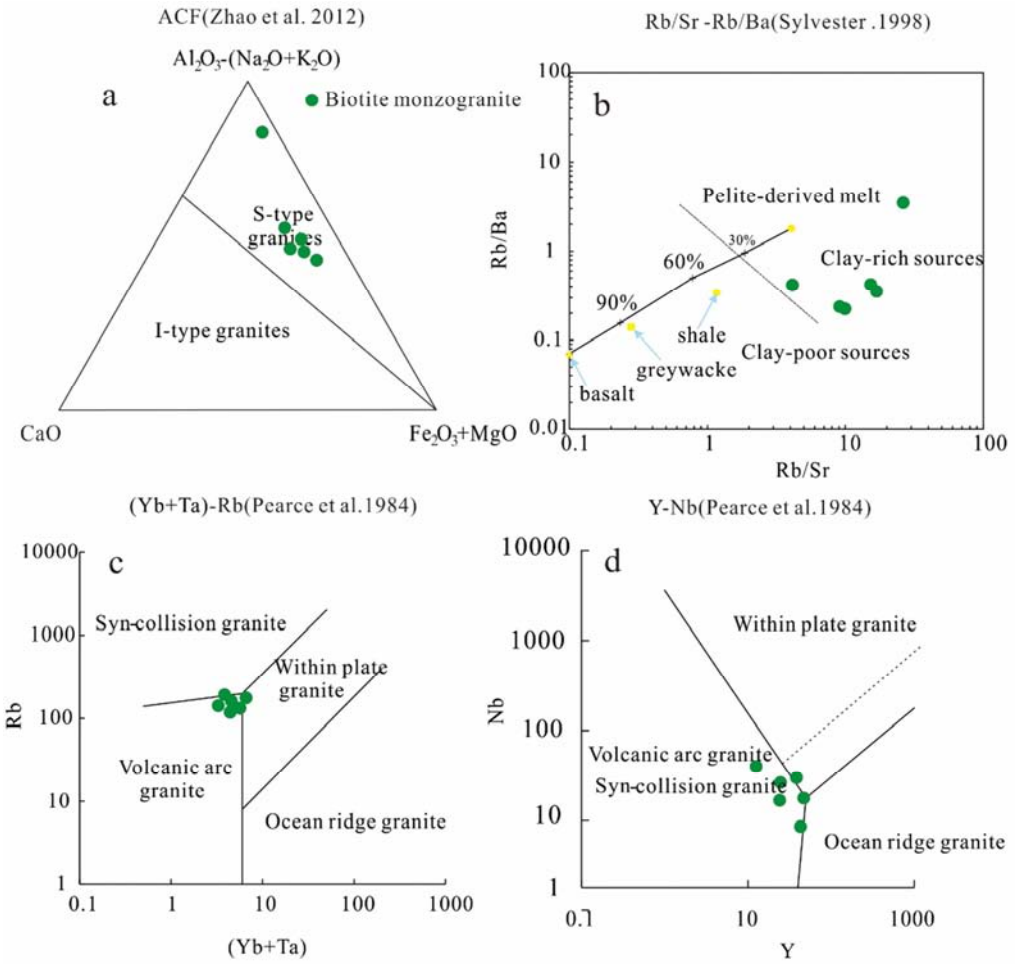


***Figure 6.*** *Illustrations of genesis and tectonic setting [11, 14, 19].*

## 6. Conclusion

Darongshan biotite monzogranite has a diagenetic crystallization age of 250.1±1.6 Ma. It was formed during the Early Triassic period and is the product of early Indosinian magmatic activity. Geochemical analyses suggested that the Darongshan biotite monzonite shows a weak Eu negative anomaly (δEu= 0.13-0.57) and decreased HREE; it has undergone a highly differentiated evolution. The Darongshan biotite monzogranite exhibited significant negative anomalies of HFSE (Nb, Ta, Ti, and P) and significant positive anomalies of LILE (Rb, Th, U, and Pb). According to the study, the Darongshan biotite monzogranite is an S-type granite, and its source material comes from the remelting of ancient crustal material. Its granite was formed in the island arc environment of oceanic subduction and orogenic stage, further confirming the geological records of the remaining Qinfang oceanic basin.

## References

[1] Chappell B W (1999). Aluminium Saturation in I- and S-Type Granites and the Characterization of Fractionated Haplogranites. Lithos, 46 (3): 535-551.

[2] Deng X G, Chen Z G, Li X H (2004). Shrimp U-Pb Zircon Dating of the Darongshan—Shiwandashan Granitoid Belt in Southeastern Guangxi, China. Geological Review, 50 (4): 426-432.

[3] Irvine T N, Baragar W R A (1971). A Guide to the Chemical Classification of the Common Volcanic Rocks. Canadian Journal of Earth Sciences, 8 (5): 523-548.

[4] Jiao S J, Guo J H, Peng S B (2013). Petrogenesis of Garnet in the DarongshanShiwandashan Granitic Suite of the South China Block and the Metamorphism of the Granulite Enclave. Acta Petrologica Sinica, 29: 1740-1758.

[5] Kun L, Wancai S, Fei D (2017). The Petrology, Geochemical Characteristics and Origin of the Napeng Granite Mass Formed in Indo-China Period in the West of Guangdong Province. Journal of Geomechanics, 23 (3): 411-421.

[6] Li Z X, Li X H (2007). Formation of the 1300-km-Wide Intracontinental Orogen and Postorogenic Magmatic Province in Mesozoic South China: A Flat-Slab Subductior Model. Geology, 35 (2): 179-182.

[7] Li Y, Wei J, Santosh M, Tan J, Fu L, Zhao S (2016). Geochronology and Petrogenesis of Middle Permian S-Type Granitoid in Southeastern Guangxi Province, South China: Implications for Closure of the Eastern Paleo-Tethys. Tectonophysics, 682: 1-16.

[8] Jochum K P, McDonough W F, Palme H, Spettel B (1989). Compositional Constraints on the Continental Lithospheric Mantle from Trace Elements in Spinel Peridotite Xenoliths. Nature, 340 (6234): 548-550.

[9] Maniar P D, Piccoli P M (1989). Tectonic Discrimination of Granitoids. Geological Society of America Bulletin. Geological Society of America Bulletin, 101 (5): 635-643.

[10] Nockolds S R, Allen R (1956). The Geochemistry of Some Igneous Rock Series—III. Geochimica et Cosmochimica Acta, 9 (1-2): 34-77.

[11] Pearce J A, Harris N B W, Tindle A G (1984). Trace Element Discrimination Diagrams for the Tectonic Interpretation of Granitic Rocks. Journal of Petrology, 25 (4): 956-983.

[12] Yuanxi Q, Huanjiang C (1993). Professional Papers for the Gcological Structure of Yunkaidashan and Its Adjacent Areas. Beijing: Geological Publishing House.

[13] Sun S S, McDonough W F (1989). Chemical and Isotope Systematics of Oceanic Basalts Implications for Mantle Composition and Processes. In Saunders AD, Ed Magmatism in Ocean Basins. Geological Society London Special Publications, 42: 313, 3456.

[14] Sylvester P J (1998). Poat-Collisional Strongly Peraluminous Granites. Lithos, 45 (1-4): 29-44.

[15] Taylor S R, McLennan S M (1985). The Continental Crust: Its Composition and Evolution. Oxford: Blackwell.

[16] Mengyu T, Di Yongjun W S, Yilong J (2021). Geochemical Characteristics and Genesis of Biotite Monzogranite in Napeng Granite in Yunkai Area. Journal of Jilin University (Earth Science Edition), 51 (3): 749-766.

[17] Wang C, Liang X Q, Zhou Y, Fu J G, Jiang Y, Dong C G, Xie Y H, Tong C X, Pei J X, Liu P (2015). Construction of Age Frequencies of Provenances on the Eastern Side of the Yinggehai basin: Studies of LA-ICP-MS U–Pb Ages of Detrital Zircons From Six Modern Rivers, Western Hainan, China. Earth Science Frontiers, 22: 277-289.

[18] Xiaofeng Q, Zongqi W, Jie C, Zuohai F, Guiang H, Luozhong P (2013). Petrogenesis of Early Indosinian Granites From the Southwestern Segment of Qinfang Tectonic Belt, Southern Guangxi: Constraints From Zircon u-pb Chronology and Geochemistry. Journal of Jilin University (Earth Science Edition), 43 (5): 1471-1488.

[19] Yang J H, Cawood P A, Du Y (2012b). Detrital record of Indosinian mountain building in SW China: provenance of the Middle Triassic turbidites in the Youjiang Basin. S, Huang H, Hu L S. Tectonophysics, 574-575: 105-117.

[20] Wang Y, Fan W, Zhang G, Zhang Y (2013). Phanerozoic Tectonics of the South China Block: Key Observations and Controversies. Gondwana Research, 23 (4): 1273-1305.

[21] Zhao L, Guo F, Fan W M, Li C W, Qin X F, Li H X (2012). Origin of the Granulite Enclaves in Indo-Sinian Peraluminous Granites, South China and Its Implication for Crustal Anatexis. Lithos, 150: 209-226.

[22] Zhou X, Chen P, Xu X (2007). The Lithosphere Dynamical Evolution of Late Mesozoic Granites in Nanling Area, Beijing: Science Press.